

FSI SIMULATION OF AN AXIALLY MOVING FLEXIBLE CYLINDER ENTRAINED BY A SUPERSONIC FLOW

LUCAS DELCOUR^{*,1}, LIEVA VAN LANGENHOVE² AND JORIS
DEGROOTE^{1,3}

¹Ghent University
Department of Flow, Heat and Combustion Mechanics
Sint-Pietersnieuwstraat 41, 9000 Ghent, Belgium
e-mail: lucas.delcour@ugent.be, web page: <http://www.ugent.be/ea/floheacom>

²Ghent University, Centre for Textile Science and Engineering, Department of Materials,
Textiles and Chemical Engineering
Technologiepark 907, 9052 Zwijnaarde (Ghent), Belgium
web page: <http://www.ugent.be/ea/match>

³Flanders Make, Belgium

Key words: Air jet weaving, Fluid-structure interaction, Supersonic flow, Chimera

Abstract. Air jet weaving looms are widely used to weave fabrics because of the high production speed that can be attained. This is directly linked to the high insertion speed of the yarns. The yarn is accelerated into the reed by a main nozzle and its motion is subsequently supported by underexpanded jets emanating from relay nozzles. The contact with the reed is the only mechanical guidance that the yarn experiences along its path and its motion depends heavily on its interaction with the air flow. The yarn can thus deviate from its envisaged path and cause a failed insertion. Furthermore, the tension in the yarn, induced by the traction of the air and the inertia and resistance of mechanical components, can cause yarn breakage. Failed insertions and broken yarns are undesired as they require the machine to be restarted.

Due to the high speed of the yarn and the mechanical components, optical accessibility to the yarn inside the main nozzle is very limited. Furthermore, the complex geometry experienced by the air flow makes it hard to assess the influence of adaptations. Fluid-structure interaction (FSI) simulations might assist in understanding the behaviour of the air flow and the yarn. However, the flexibility of the yarn in combination with the high speed flow presents its own challenges.

In this research an attempt is made to simulate the launch of a yarn by a single main nozzle into the atmosphere. To better approximate reality, the yarn is considered to be stored on a drum in front of the nozzle. A two-way fluid-structure interaction simulation

is performed using Fluent for the flow side, Abaqus for the structural side and the in-house code Tango for the coupling. Continuum elements or beam elements are used for the structure. The axial motion and large transversal displacement of the yarn pose significant challenges for a single deforming grid in the flow solver. To avoid these complications a Chimera approach, which superimposes several meshes, is opted for.

The FSI simulations show that the yarn can indeed be represented by beam elements. The gain in computational time by switching to beam elements is evaluated and the results from the FSI calculation are compared to experimental results in terms of yarn velocity. Stresses in the yarn are examined to identify high tension regions.

1 INTRODUCTION

A machine used to weave a fabric is called a weaving loom. A general weaving process can basically be broken down into a repetition of 3 actions to insert a weft/pick (along the width of the fabric) in between the warp threads (along the length of the fabric):

1. Shedding: The warp threads are separated into 2 groups, an upper and a lower one. During the shedding phase the upper and lower group interchanged. This locks the previously inserted weft into the cloth and creates a space for the next insertion.
2. Picking: The weft is launched through the space created in the shedding phase.
3. Beating-Up: The inserted weft is pushed against the rest of the cloth by the reed.

Weaving looms are categorized based on their method of insertion. In the earliest weaving looms, a shuttle was used to propel the weft across the loom. Therefore, these machines are referred to as shuttle weaving looms. More modern alternatives are rapier looms (using hooks to transport the yarn) and air or water jet looms.

The simulation performed in this research is related to the field of air jet weaving looms. In such looms the yarn is accelerated by a main nozzle which generates a supersonic flow. Along its path the yarn motion is supported by auxiliary (relay) nozzles. The air flow from those nozzles is channeled by the reed which consists of a series of profiled lamellae that form a half-open tunnel. During its flight the weft is not constrained mechanically (except by possible contact with the reed). If the air flow is not tuned correctly it can cause the yarn to be blown out of the channel. Additionally, a too strong acceleration of the yarn or too abrupt braking can cause damage to the yarn. Both of the previously mentioned phenomena lead to a failed insertion requiring the bad insertion to be removed and the process to be restarted. Especially for air jet weaving looms these stops of the machine are undesirable as their high production speed is one of their key aspects. Figure 1 shows a schematic overview of an air-jet weaving machine with an open-profile reed.

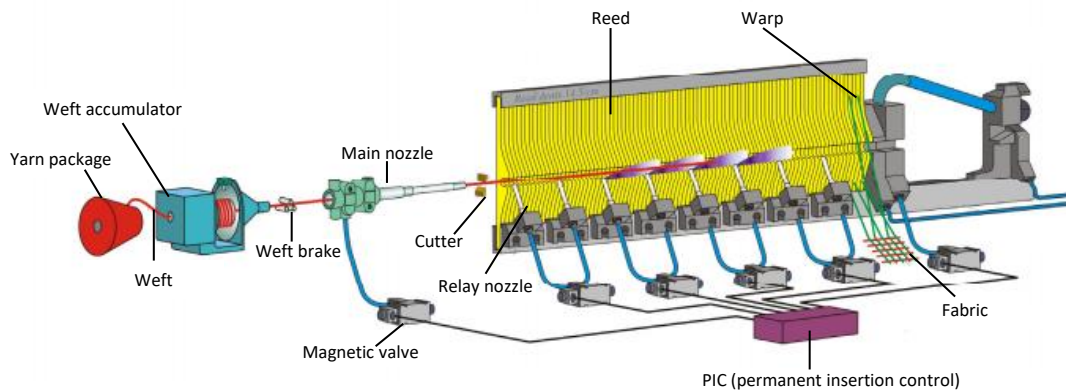


Figure 1: Schematic overview of an air-jet weaving machine with an open-profile reed (adapted from Szabó and Szabó¹)

Throughout the years several methods have been employed to analyze the motion of the weft or more generally the behavior of a fiber in air flow. One of the first to perform research into this topic was Uno.² He established an equation of motion for a weft which was assumed to travel along a straight path on the centerline. For the aerodynamic forces he relied on an approximate formula for the centerline velocity decay of a jet and aerodynamic force coefficients. Similar methods were employed by Salama et al.³ and Szabó et al.⁴ Salama investigated the use of regular and slotted tubes for insertion, while Szabó focussed on the use of confusor drop wires. In confusor drop wire systems the air channel is formed by a series of circular openings whose circumference is not entirely closed. This allows for a better confinement of the air flow but limits the weaving width and warp density. Adanur and Mohamed⁵ used a similar model to compare the tension experienced by the yarn during launch for several storage systems. Later on, Celik et al.⁶ established a model for air jet weaving looms that also use relay nozzles to support the yarn motion.

Tang and Advani⁷ were among the first to employ computational mechanics on high aspect ratio fibers. They performed simulations for a single fiber and for 2 interacting fibers in a simple shear flow. As the structural motion does not influence the flow field the simulations can be classified as a one-way coupled simulation. De Meulemeester, Githaiga et al.⁸ used computational fluid dynamics (CFD) to calculate the flow field inside a main nozzle. A snapshot of this flow field was used to calculate the force on the yarn (using force coefficients). These forces were then passed to a 1D structural model to analyse the tension in the yarn during braking. A 3D extension of the model was then used by De Meulemeester, Puissant et al.⁹ to numerically simulate the unwinding of a yarn from a drum by a main nozzle. Battochio et al.¹⁰ similarly used a one-way coupling approach for simulating the motion of a long flexible fiber in a uniform turbulent flow field with an average velocity of 10 m/s. Kondora¹¹ employed one-way coupled simulations to obtain

the probability distribution function of fiber orientation in the converging channel of a papermachine headbox.

In a one-way coupling the influence of yarn motion on the flow is neglected. In some cases this interaction can have a noticeable effect on the dynamics. To capture these effects, a two-way coupling approach has to be employed resulting in fluid-structure interaction (FSI). Zeng et al.¹² performed 2D two-way coupled FSI simulations inside the nozzle of an air-jet spinning machine. Similarly, Pei and Yu¹³ simulated the fiber motion in a Murata Vortex Spinning machine. Another 2D two-way FSI simulation was performed by Wu et al.¹⁴ who investigated the yarn whipping of a weft protruding from the main nozzle in an air-jet weaving loom. Osman, Malengier et al.¹⁵ used an immersed boundary method to perform FSI simulations for a weft launched by a main nozzle. The flow simulations were performed in a 2D-axisymmetric framework. As a structural solver an extension of the model of De Meulemeester, Puissant et al.⁹ was used. Following this work, Osman, Delcour et al.¹⁶ used a 3D model to simulate the oscillatory behavior of a yarn, which was clamped at the yarn inlet, inside the main nozzle. The simulation duration was, however, limited due to mesh degradation as a single deforming grid was used. In this research an attempt is made to perform a 3D two-way coupled FSI simulation of a weft, initially stored on a drum, launched into the atmosphere by a main nozzle. A Chimera technique is used to overcome the problem of mesh degradation and to facilitate the incorporation of axial yarn motion. In a Chimera technique several meshes are superimposed and the solution is obtained by interpolation between overlapping meshes. For the case at hand, a fixed background grid is used for the flow domain. On top of that a mesh containing the yarn, referred to as the component mesh, is superimposed. The component mesh moves along with the yarn but is not limited by the boundaries of the flow domain. Consequently, large yarn deformations do not severely degrade the mesh quality.

2 Methodology

2.1 Structural model

Figure 2 displays the structural model. It contains an analytical rigid body representing the main nozzle with a funnel-like attachment to guide the yarn into the nozzle. The flexible yarn itself consists of 65000 C3D8 elements (3D continuum with 8 nodes per element). The yarn is represented as if it were wound on a drum in front of the main nozzle. The drum itself has not been included in the model.

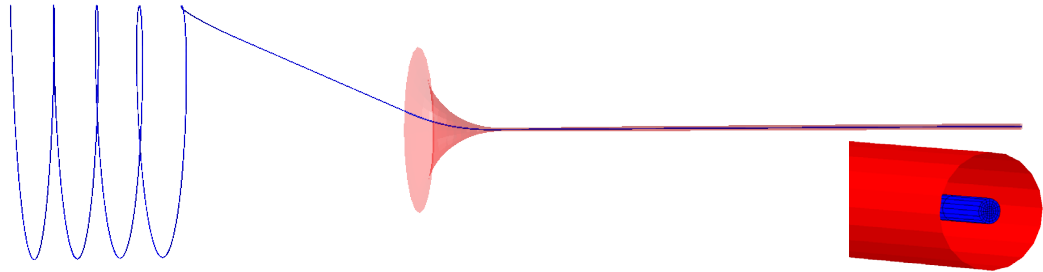


Figure 2: Structural model consisting of the flexible yarn (blue) and the rigid main nozzle (red).

The radial dimensions of the analytical rigid body are 15% smaller than the actual nozzle geometry and contact between the yarn and the nozzle wall is taken into account. This ensures that there is always sufficient space in between the yarn and nozzle wall in the flow solver. The physical properties of the yarn correspond to those of a nylon yarn ($E = 2.5$ GPa, $\nu = 0.3$, linear density = 464 g/km, $D = 0.72$ mm). At the start of the winding (left end of Figure 2) the yarn is considered clamped; the right end of the yarn is free. The normal component of the contact between the yarn and the nozzle is modeled as a hard contact using a linear penalty method, which imposes a contact force proportional to the penetration distance. No friction between the nozzle and the yarn is considered so the tangential component of the contact force is set to 0. The time step size is generally the same as the one used in the flow solver. Whipping behavior of the yarn resulting in a high-speed impact between the yarn and the nozzle can, however, destabilize the structural solver. When convergence problems are encountered in the structural solver, its time step is temporarily reduced using subcycling in the structural solver. The structural simulations are performed with Abaqus 6.14.

2.2 Flow model

As mentioned in the introduction a Chimera approach is opted for. This implies that multiple meshes are superimposed in the flow solver. In this case a single background and single component grid are employed. The background grid remains fixed while the component grid deforms along with the yarn. The flow model is entirely 3-dimensional.

Figure 3 displays the background grid and its boundary conditions. This grid consists of approximately 500 000 hexahedral cells. Axial and radial expansion ratios are employed to reduce the total number of cells and as such the required computational time. In the circumferential direction 40, equally spaced, subdivisions are employed. The highest mesh densities are located in the shock region and at the exit of the nozzle.

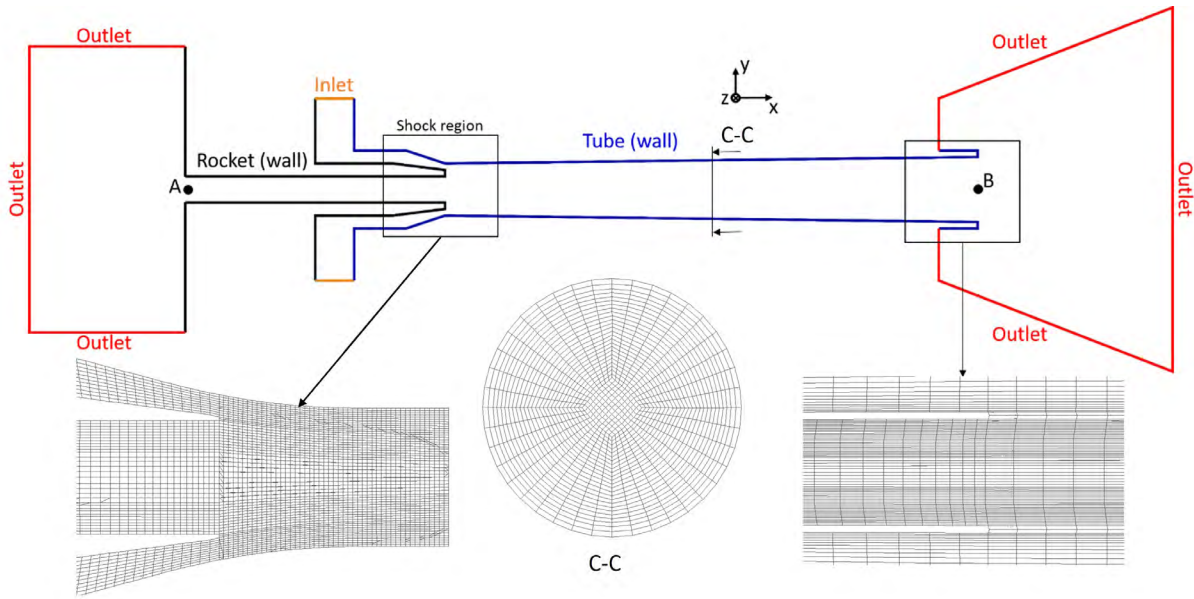


Figure 3: Background mesh and the associated boundary conditions. At the “Inlet” a value for the total pressure is imposed; at the “Outlet” a value for the static pressure is imposed.

The component mesh consists of a bent cylinder of diameter 2 mm whose centerline coincides with that of the yarn. The component mesh contains approximately 3.8 million hexahedral cells. A uniform axial and circumferential spacing is applied together with a slight radial bias. Figure 4 shows a simplified representation of the component mesh. At the start of the simulation the points A and B in Figure 4 coincide with the points A and B in Figure 3, respectively. The dashed lines in Figure 4 indicate the left outlet of the background mesh. As can be seen a large part of the component mesh is, thus, located outside of the actual computational domain. During the calculation these cells are disabled. The force on the part of the yarn located outside of the computational domain is calculated under the assumption that the pressure on the surface is uniform and equal to atmospheric pressure, the viscous force on that part is obtained from the law of the wall with a flow velocity of 0 m/s and a wall velocity as obtained from the structural solver.

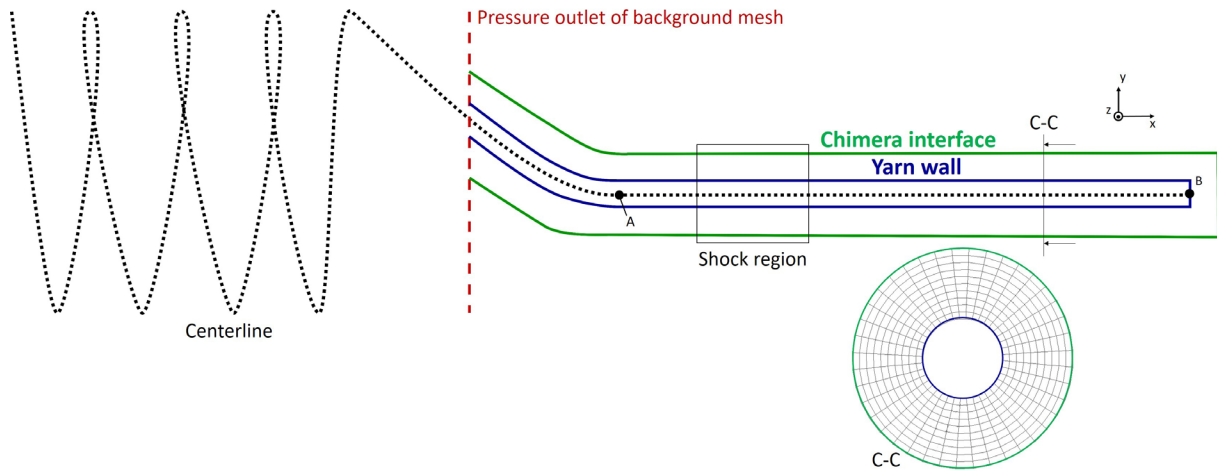


Figure 4: Component mesh and its associated boundary conditions. Initially points A and B coincide with those in Figure 3. The dashed lines indicate the left outlet of the background mesh.

The component mesh, delimited by the Chimera interface, moves along with the yarn. For the mesh deformation a spring-based smoothing method without damping is used, implying that all edges have an identical spring stiffness. Large rotational motions can introduce some skew into the cells but for the simulation at hand this was observed to be within acceptable limits. The turbulent simulations are performed with the $k-\omega$ SST model. A first-order implicit time stepping scheme was employed with a time step size of $5e-06$ s. The flow was initialized as a stationary flow. At the inlet a total pressure of 4.7 bar gauge was imposed (to save on computational time the pressure build-up phase was not considered). The value for the total pressure was obtained from experimental measurements. The flow simulations are performed with Fluent 18.2.

2.3 Coupling

The flow and structural solvers are coupled using an in-house code named “Tango” which employs a partitioned approach. The coupling is implicit, using a Gauss-Seidel procedure as this converges quickly for this case. A coupling iteration is considered to be converged when the vector norm for the displacement of all interface nodes relative to the previous iteration becomes smaller than 10^{-6} m.

3 Simulation results

Using the above methodology a simulation was executed over a period of 3350 time steps (for the first 900 time steps a time step size of $1e-05$ s was used). This was sufficient for the yarn tip to reach the end of the flow domain (located at 0.5 m downstream of the yarn inlet). Figure 5 shows the centerline position of the yarn at several time instants. The simulation could be continued in time without changes to the model. Forces on the

section of the yarn that exited the domain are then obtained by considering the flow variables in the wall adjacent cells to be frozen at their final value. Alternatively, a mesh section could be appended to the end of the domain or the simulation could be restarted with a longer flow domain.

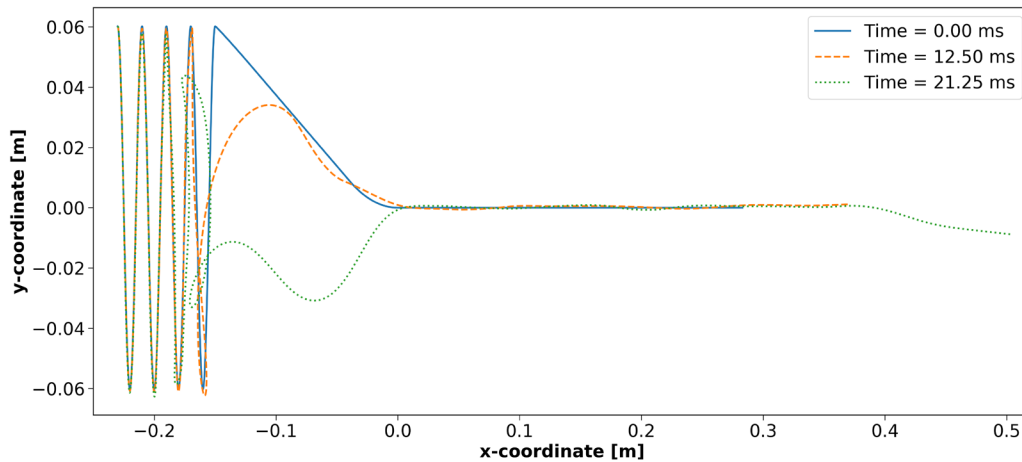


Figure 5: Centerline position of the yarn at several time instants.

In Figure 6 the x(axial)-, y- and z-coordinates of the yarn tip are plotted as a function of time. The tip displays a smooth axial motion; the dashed line indicates the end of the flow domain. An oscillation can be observed in both the y- and z-directions. Towards the end of the simulation the tip starts drooping off due to gravity (which works in the negative y-direction). From the x-displacement of the yarn tip a tip velocity can be extracted, which could be compared with experiments given a suitable setup. The velocity as obtained from the displacement is plotted in Figure 7. Initially the yarn tip displays a rather linear velocity increase, towards the end of the simulation the velocity starts leveling off at about 16 m/s.

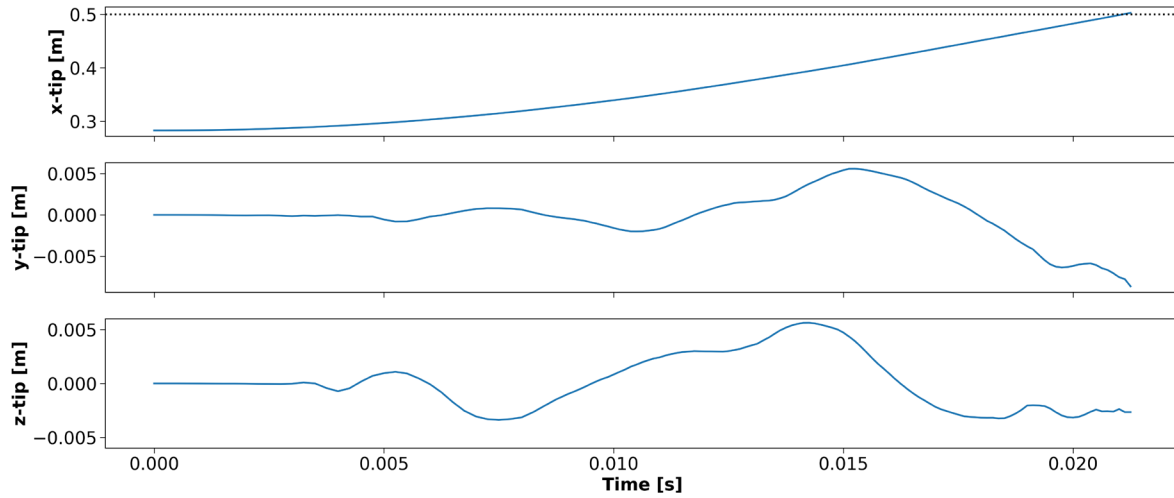


Figure 6: Position of the yarn tip as a function of time.

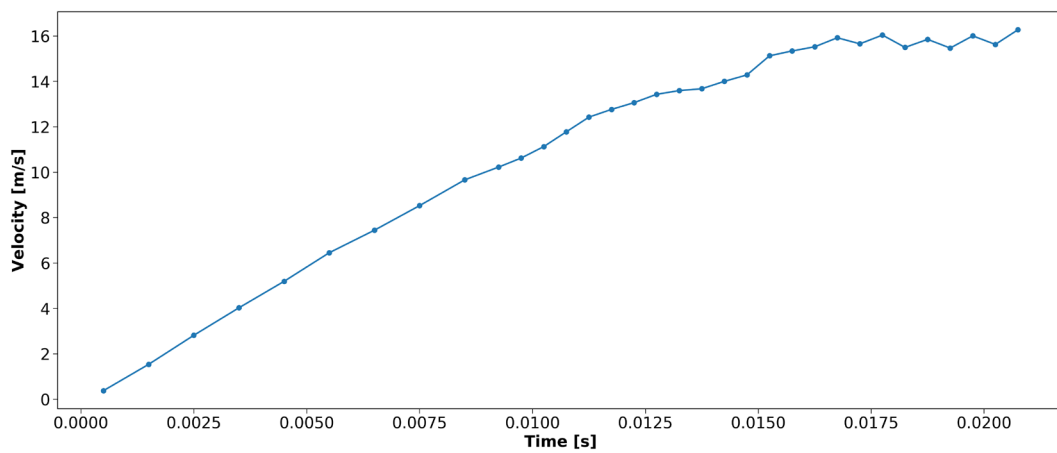


Figure 7: Axial tip velocity as obtained from the simulation.

From the structural solver, data about the stresses in the material can be obtained. Figure 8 shows the maximum Von Mises stress in the yarn over time. A maximum stress of 52.3 MPa was recorded. This force can be traced back to an abrupt contact between the yarn and the funnel. Later on the location of the maximum stress value relocates to the jet entrance. A contour plot of the Von Mises stress, extrapolated to the surface nodes, at the end of the simulation is displayed in Figure 9. Due to the extrapolation the values cannot directly be compared to those in Figure 8.

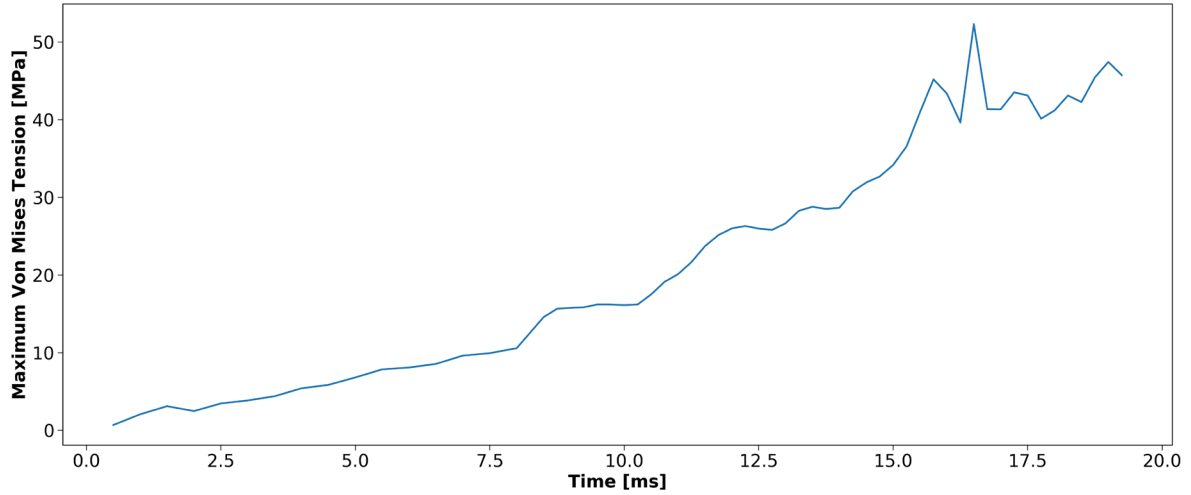


Figure 8: Maximal Von Mises stress observed in the elements of the yarn as a function of time.

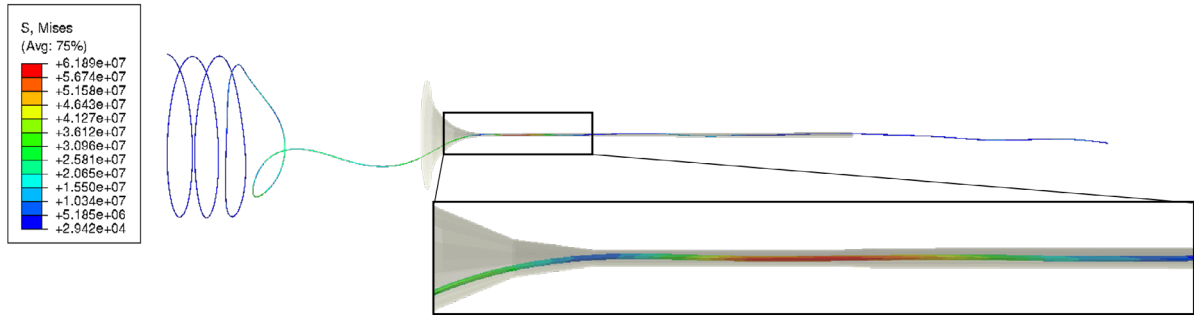


Figure 9: Von Mises stress extrapolated to the nodes at the final time step of the simulation.

4 Computational time

The largest part of the simulation was performed on the HPC-UGent infrastructure. 42 cores were assigned to the flow solver and 4 to the structural solver. The simulation had an average rate of 75 time steps per day with, on average, 2 coupling iterations per time step. This implies a total simulation time of approximately 40 days. About 70% of the time was consumed by the flow solver and 15% by the structural solver. The remainder of the time is related to the coupling and data transfer.

As the structure has a uniform cross section and a high aspect ratio, it lends itself well to the use of beam elements. This can simplify the structural model and reduce the computational cost. A preliminary test showed that beam elements are indeed suited for the structural model and that the computational time could be reduced by approximately 10% by doing so.

5 Conclusion

In this research a Chimera technique was employed to simulate the launch of a yarn by a main nozzle of an air-jet weaving loom. The Chimera technique allows large yarn deformations and axial motion to be accommodated for without severely degrading the mesh quality. Information about e.g. yarn velocity, tip displacements and stresses can be extracted from the simulation. The simulation, however, has a large computational cost. One possibility of reducing the cost is switching the structural model from continuum elements to beam elements. A gain of 10% in computational time can be attained by doing so.

6 Acknowledgments

The computational resources (Stevin Supercomputer Infrastructure) and services used in this work were provided by the VSC (Flemish Supercomputer Center), funded by Ghent University, FWO and the Flemish Government department EWI.

REFERENCES

- [1] Szabó, L. and Szabó, L. Weft insertion through open profile reed in air jet looms. *Annals of faculty engineering Hunedoara, International journal of engineering*. (2012) **ISSN(1584-2665)**:211-218.
- [2] Uno, M. A study on air-jet loom with substreams added, Part 1: Deriving the equation of motion for weft. *Journal of the Textile Machinery Society of Japan*. (1972) **25**:48–56.
- [3] Salama, M. Adanur, S. and Mohamed, M.H. Mechanics of a single nozzle air-jet filling insertion system, Part III: Yarn insertion through tubes. *Textile Research Journal*. (1987) **57**:44–54.
- [4] Szabó, L. Patkó, I. and Oroszlány, G. The dynamic study of the weft insertion of air jet weaving machines. *Acta Polytechnica Hungarica*. (2010) **7**:93–107.
- [5] Adanur, S. and Mohamed, M.H. Analysis of yarn tension in air-jet filling insertion. *Textile Research Journal*. (1991) **61**:259–266.
- [6] Celik, N. Babaarslan, O. and Bandara, M.P.U. A mathematical model for numerical simulation of weft insertion on air-jet weaving machine. *Textile Research Journal*. (2004) **74**:236–240.
- [7] Tang, W. and Advani, S. Dynamic simulation of long flexible fibers in shear flow. *CMES*. (2005) **8**:165–176.
- [8] De Meulemeester, S. Githaiga, J. Van Langenhove, L. et al. Simulation of the dynamic yarn behavior on airjet looms. *Textile Research Journal*. (2005) **75**:724–730.

- [9] De Meulemeester, S. Puissant, P. and Van Langenhove, L. Three-dimensional simulation of the dynamic yarn behavior on air-jet looms. *Textile Research Journal*. (2009) **79**:1706–1714.
- [10] Battocchio, F. Sutcliffe, M.P.F. and Teschner, F. Dynamic simulation of long polymeric fibres immersed in a turbulent air flow. *In: Proceedings of the IMSD2012 - The 2nd Joint International Conference on Multibody System Dynamics, Stuttgart, Germany, 29 May - 1 June 2012*. <http://www2.eng.cam.ac.uk/~mpfs/papers/BST2012FibreTurbulentIMSD.pdf>.
- [11] Kondora, G. and Asendrych, D. Modelling of the dynamics of flexible and rigid fibres. *Chemical and Process Engineering*. (2013) **34**:87–100.
- [12] Zeng, Y.C. Yang, J.P. and Yu, C.W. Mixed Euler-Lagrange approach to modeling fiber motion in high speed air flow. *Applied Mathematical Modelling*. (2005) **29**:253–261.
- [13] Pei, Z. and Yu, C. Numerical study on the effect of nozzle pressure and yarn delivery speed on the fiber motion in the nozzle of Murata vortex spinning. *Journal of Fluids and Structures*. (2011) **27**:121–133.
- [14] Wu, Z. Chen, S. Liu, Y. et al. Air-flow characteristics and yarn whipping during start-up stage of air-jet weft insertion. *Textile Research Journal*. (2016) **86**:1988–1999.
- [15] Osman, A. Malengier, B. De Meulemeester, S. et al. Simulation of air flow-yarn interaction inside the main nozzle of an air jet loom. *Textile Research Journal*. (2017) **88**:1173–1183.
- [16] Osman, A. Delcour, L. Hertens, I. et al. Toward three-dimensional modeling of the interaction between the air flow and a clamped-free yarn inside the main nozzle of an air jet loom. *Textile Research Journal*. (2019) **89**:914–925.